ORGANOMETALLICS
Article

Organometallics **2010,** *29,* 6201–6208 6201
DOI: 10.1021/om100495e

Alkali Metal Complexes of a *tert*-Butylphosphine-Bridged Biphenolate Ligand

Yu-Lin Hsu and Lan-Chang Liang*

Department of Chemistry and Center for Nanoscience & Nanotechnology, National Sun Yat-sen University, Kaohsiung 80424, Taiwan, Republic of China

Received May 19, 2010

The coordination chemistry of group 1 metals with a potentially tridentate, dianionic biphenolate phosphine ligand that carries a phosphorus-bound *tert*-butyl group is described. Deprotonation of bis(3,5-di-*tert*-butyl-2-hydroxyphenyl)-*tert*-butylphosphine (H_2[^{t}Bu-OPO]) with two equivalents of *n*-BuLi, NaH, or KH in ethereal solutions produces the corresponding alkali metal complexes $\{[^t\text{Bu-OPO}]M_2(\text{solv})_x\}_2$ (M = Li, Na, K; solv = DME, THF). An X-ray diffraction study of the lithium derivative reveals a dimeric structure that contains two [^{t}Bu-OPO]Li_2(DME) units linked by two dative O−Li bonds; the two lithium atoms in each monomeric [^{t}Bu-OPO]Li_2(DME) are bridged by both phenolate oxygen donors with only one lithium being coordinated to the phosphorus donor. As a result, the Li_4O_4 moiety in $\{[^t\text{Bu-OPO}]Li_2\}_2$ constitutes three successive Li_2O_2 tetragons fused in an open cubane structure. The coordination of the phosphorus donor to lithium in $\{[^t\text{Bu-OPO}]Li_2(\text{DME})\}_2$ is also confirmed by variable-temperature $^{31}P\{^1H\}$ and $^7Li\{^1H\}$ NMR studies. Interestingly, the sodium complex is composed of two [^{t}Bu-OPO]Na_2(DME)$_2$ units linked by a bridging DME; each [^{t}Bu-OPO]Na_2(DME)$_2$ subunit is structurally similar to its lithium analogue though adopting one more coordinated DME. The potassium complex also contains two [^{t}Bu-OPO]K_2(THF)$_2$ moieties linked with two dative O−K bridges; the structure of the monomeric [^{t}Bu-OPO]K_2(THF)$_2$ unit, however, is markedly distinct from those of its lighter congeners. In addition to the anticipated *fac*-coordination from the heteroatoms in the biphenolate phosphine ligand, one of the potassium atoms in monomeric [^{t}Bu-OPO]K_2(THF)$_2$ is π-bound to one of the aryl rings incorporated in the [^{t}Bu-OPO]$^{2-}$ backbone.

Introduction

Alkali metal complexes are ubiquitous in organic and inorganic syntheses. They are usually used as starting materials for deprotonation, nucleophilic addition, metathetical reactions, etc.[1,2] Their unique reactivity also makes them an attractive candidate as initiators for polymer preparation.[3−6] For instance, lithium aggregates containing alkoxides and/or aryloxides have shown remarkable activity in ring-opening polymerization (ROP) of cyclic molecules and, in some cases, in a controlled manner.[7]

We are currently investigating reaction chemistry involving metal complexes of hybrid chelating ligands.[8−12] In particular, a series of group 1, 4, 5, and 14 derivatives of a biphenolate phosphine ligand, [PhP(3,5-^{t}Bu$_2$C$_6$H$_2$-2-O)$_2$]$^{2-}$ ([Ph-OPO]$^{2-}$), have been prepared.[13−16] This particular ligand falls into the category of current interest in chelating biphenolate ancillary design, in which not only can the aryl substituents be readily modified for steric and electronic tuning but the ways to link the two phenolate rings are also versatile.[17−29] As a result, rich

*To whom correspondence should be addressed. E-mail: lcliang@mail.nsysu.edu.tw.

(1) Seyferth, D. *Organometallics* **2006**, *25*, 2–24.
(2) Seyferth, D. *Organometallics* **2009**, *28*, 2–33.
(3) Foster, F. C.; Binder, J. L. In *Handling and Uses of the Alkali Metals*; American Chemical Society: Washington, DC, 1957; pp 26−33.
(4) Quirk, R. P.; Seung, N. S. In *Ring-Opening Polymerization: Kinetics, Mechanisms, and Synthesis*; McGrath, J. E., Ed.; American Chemical Society: Washington, DC, 1985; pp 37−45.
(5) Morton, M.; Wu, M. In *Ring-Opening Polymerization: Kinetics, Mechanisms, and Synthesis*; McGrath, J. E., Ed.; American Chemical Society: Washington, DC, 1985; pp 175−182.
(6) Kelley, D. J.; Tobolsky, A. V. *J. Am. Chem. Soc.* **1959**, *81*, 1597–1600.
(7) Sutar, A. K.; Maharana, T.; Dutta, S.; Chen, C.-T.; Lin, C.-C. *Chem. Soc. Rev.* **2010**, *39*, 1724–1746.
(8) Liang, L.-C. *Coord. Chem. Rev.* **2006**, *250*, 1152–1177.
(9) Liang, L.-C.; Chien, P.-S.; Huang, Y.-L. *J. Am. Chem. Soc.* **2006**, *128*, 15562–15563.
(10) Liang, L.-C.; Lin, J.-M.; Lee, W.-Y. *Chem. Commun.* **2005**, 2462–2464.
(11) Liang, L.-C.; Chien, P.-S.; Lee, P.-Y. *Organometallics* **2008**, *27*, 3082–3093.
(12) Liang, L.-C.; Lin, J.-M.; Hung, C.-H. *Organometallics* **2003**, *22*, 3007–3009.
(13) Chang, Y.-N.; Liang, L.-C. *Inorg. Chim. Acta* **2007**, *360*, 136–142.
(14) Liang, L.-C.; Chang, Y.-N.; Lee, H. M. *Inorg. Chem.* **2007**, *46*, 2666–2673.
(15) Liang, L.-C.; Cheng, L.-C.; Tsai, T.-L.; Hu, C.-H.; Guo, W.-H. *Inorg. Chem.* **2009**, *48*, 5697–5703.
(16) Liang, L.-C.; Chang, Y.-N.; Chen, H.-S.; Lee, H. M. *Inorg. Chem.* **2007**, *46*, 7587–7593.
(17) Alexander, J. B.; La, D. S.; Cefalo, D. R.; Hoveyda, A. H.; Schrock, R. R. *J. Am. Chem. Soc.* **1998**, *120*, 4041–4042.
(18) Zhu, S. S.; Cefalo, D. R.; La, D. S.; Jamieson, J. Y.; Davis, W. M.; Hoveyda, A. H.; Schrock, R. R. *J. Am. Chem. Soc.* **1999**, *121*, 8251–8259.
(19) van der Linden, A.; Schaverien, C. J.; Meijboom, N.; Ganter, C.; Orpen, A. G. *J. Am. Chem. Soc.* **1995**, *117*, 3008–3021.
(20) Kim, Y.; Jnaneshwara, G. K.; Verkade, J. G. *Inorg. Chem.* **2003**, *42*, 1437–1447.
(21) Groysman, S.; Goldberg, I.; Goldschmidt, Z.; Kol, M. *Inorg. Chem.* **2005**, *44*, 5073–5080.
(22) Segal, S.; Goldberg, I.; Kol, M. *Organometallics* **2005**, *24*, 200–202.
(23) Capacchione, C.; Proto, A.; Ebeling, H.; Mulhaupt, R.; Moller, K.; Spaniol, T. P.; Okuda, J. *J. Am. Chem. Soc.* **2003**, *125*, 4964–4965.
(24) Sernetz, F. G.; Mulhaupt, R.; Fokken, S.; Okuda, J. *Macromolecules* **1997**, *30*, 1562–1569.
(25) Fokken, S.; Spaniol, T. P.; Kang, H. C.; Massa, W.; Okuda, J. *Organometallics* **1996**, *15*, 5069–5072.

Published on Web 11/03/2010

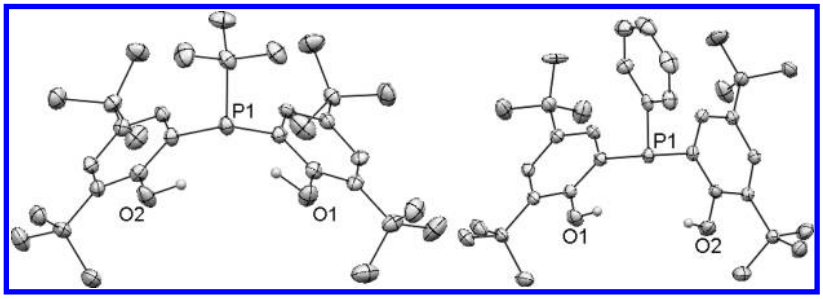

Figure 1. Molecular structures of H_2[^{t}Bu-OPO] (left) and H_2[Ph-OPO] (right) with thermal ellipsoids drawn at the 35% probability level.

structural chemistry has evolved. We have recently shown that [Ph-OPO]$^{2-}$ appears to have a strong tendency to form bis-ligated complexes with group 4 and 5 metals.[14,15] We envisioned that such propensity may perhaps be inhibited, at least to some degree, by replacing the phosphorus-bound phenyl group with a *tert*-butyl, the monoligated complexes derived from which should be more sterically demanding and less electronically deficient. Having this in mind, we have set out to prepare a *tert*-butylphosphine-bridged biphenolate ligand and pursue its coordination and reaction chemistry. In this contribution, we describe the preparation of such a ligand and its group 1 derivatives. Interestingly, these alkali metal complexes exhibit distinct structural motifs from their phosphorus-bound phenyl counterparts.[13] We note that although biphenolate phosphine ligands have been known since 1980,[30] structurally characterized alkali metal derivatives are extremely rare.[13,31]

Results and Discussion

The *tert*-butyl-substituted ligand precursor bis(3,5-di-*tert*-butyl-2-hydroxyphenyl)-*tert*-butylphosphine (H_2[^{t}Bu-OPO]) may be readily prepared with conditions similar to those of its phenyl analogue.[32] In situ lithiation of 2-bromo-4,6-di-*tert*-butylphenol with two equivalents of ^{n}BuLi in diethyl ether at −35 °C followed by addition of *tert*-butyldichlorophosphine generated, after anaerobic aqueous workup, H_2[^{t}Bu-OPO] as an off-white solid in 58% yield. Solution NMR data are indicative of C_s symmetry for this molecule. The hydroxyl protons are detected as a doublet resonance at 7.61 ppm with J_{HP} = 12 Hz. In comparison, the corresponding J_{HP} value for H_2[Ph-OPO] is 8 Hz.[32] The phosphorus atom resonates at −60 ppm, a signal that is shifted more upfield than that of H_2[Ph-OPO] (−50 ppm)[32] but consistent with what is anticipated in view of the more electron-releasing nature for a *tert*-butyl group.

In order to compare the structural parameters of H_2[^{t}Bu-OPO] and H_2[Ph-OPO], we attempted X-ray diffraction studies for both molecules. Single crystals of H_2[^{t}Bu-OPO] and H_2[Ph-OPO] were both grown from a concentrated acetonitrile solution at −35 °C. The solid-state structures are depicted in Figure 1. Selected bond distances and angles are summarized in Table 1. On the basis of geometry, bond distances, and bond angles, both molecules are virtually isostructural to each other, indicating the phosphorus substituent has little influence on the sterics of these protio ligands. The electronic effect, however, is perhaps more noticeable, as evidenced by the J_{HP} values observed for the hydroxyl protons in the ^{1}H NMR of these molecules.

Table 1. Selected Bond Distances (Å) and Angles (deg) for H_2[^{t}Bu-OPO] and H_2[Ph-OPO]

compound	H_2[^{t}Bu-OPO]	H_2[Ph-OPO]
C−O	1.374(4), 1.382(4)	1.367(3), 1.374(3)
P−C(phenolate)	1.832(4), 1.832(4)	1.829(2), 1.831(2)
P−^{t}Bu or P−Ph	1.867(4)	1.816(2)
C−P−C	105.16(17), 108.04(18), 109.84(18)	107.40(10), 106.38(10), 102.64(10)

Deprotonation of H_2[^{t}Bu-OPO] with two equivalents of ^{n}BuLi at −35 °C in a variety of solvents produced cleanly the dilithium complex as indicated by ^{31}P{^{1}H} NMR spectroscopy. Upon lithiation, the ^{31}P chemical shift moves downfield from −60 to ca. −13 ppm in nonpolar (e.g., toluene, pentane) or to ca. −22 ppm in polar solvents (e.g., DME, THF, Et_2O). We found that the most convenient method to isolate a well-defined product from these reactions is perhaps that conducted in DME solutions, from which the dilithium complex was obtained quantitatively (Scheme 1) as colorless prisms after recrystallization from pentane.

An X-ray diffraction study revealed that the lithium complex is an approximately C_2-symmetric dimer composed of two [^{t}Bu-OPO]Li_2(DME) units linked by two dative O−Li bonds (Figure 2, Table 2). The two lithium atoms in each monomeric [^{t}Bu-OPO]Li_2(DME) are bridged by both phenolate oxygen donors. As a result, the Li_4O_4 moiety in {[^{t}Bu-OPO]Li_2}$_2$ constitutes three fused Li_2O_2 tetragons in an open cubane motif. The four atoms in each Li_2O_2 tetragon are approximately coplanar, as evidenced by the corresponding torsion angles and the sum of internal angles. The dihedral angles between the central tetragon and the two peripheral ones are 133.28° and 136.73°. These wide angles are ascribable to steric congestion imposed by each monomeric moiety. The C_2 axis coincides with the normal vectors penetrating the center of the central Li_2O_2 tetragon.

In comparison with the phosphorus-bound phenyl derivative [Ph-OPO]Li_2(DME)$_2$ (Figure 3),[13] the monomeric unit in {[^{t}Bu-OPO]Li_2(DME)}$_2$ is notably short of one coordinated DME. The formation of a dimeric {[^{t}Bu-OPO]Li_2(DME)}$_2$ instead of [^{t}Bu-OPO]Li_2(DME)$_2$, however, reflects the less electron-deficient nature for monomeric [^{t}Bu-OPO]Li_2(DME) than [Ph-OPO]Li_2(DME), considering DME is a much better coordinating base than dative phenolate oxygen atoms. Such discrepancy is consistent with a recent result

(26) Takeuchi, D.; Nakamura, T.; Aida, T. *Macromolecules* **2000**, *33*, 725–729.
(27) Floriani, C.; Corazza, F.; Lesueur, W.; Chiesi-Villa, A.; Guastini, C. *Angew. Chem., Int. Ed.* **1989**, *28*, 66–67.
(28) Corazza, F.; Floriani, C.; Chiesi-Villa, A.; Guastini, C. *Inorg. Chem.* **1991**, *30*, 145–148.
(29) Ko, B.-T.; Lin, C.-C. *J. Am. Chem. Soc.* **2001**, *123*, 7973–7977.
(30) Tzschach, A.; Nietzschmann, E. *Z. Chem.* **1980**, *20*, 341–342.
(31) Carmichael, C. D.; Fryzuk, M. D. *Dalton Trans.* **2008**, 800–806.
(32) Siefert, R.; Weyhermuller, T.; Chaudhuri, P. *J. Chem. Soc., Dalton Trans.* **2000**, 4656–4663.

Scheme 1

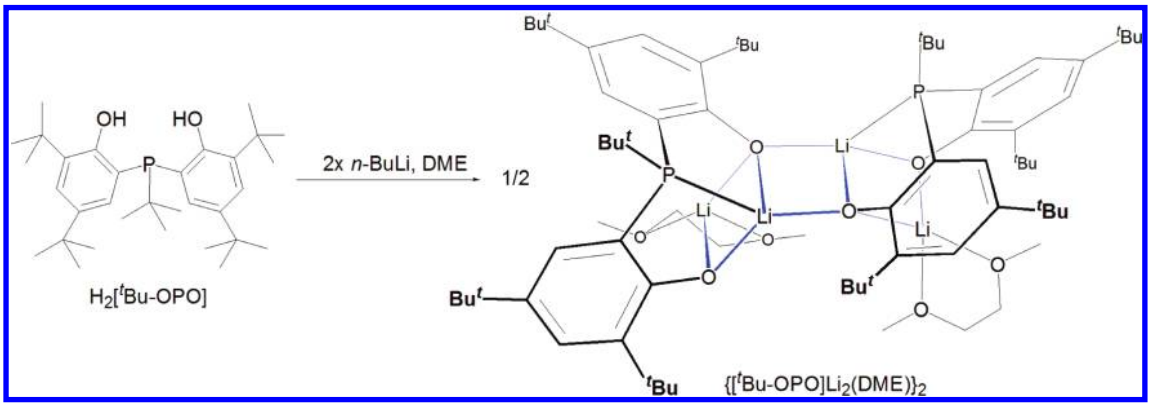

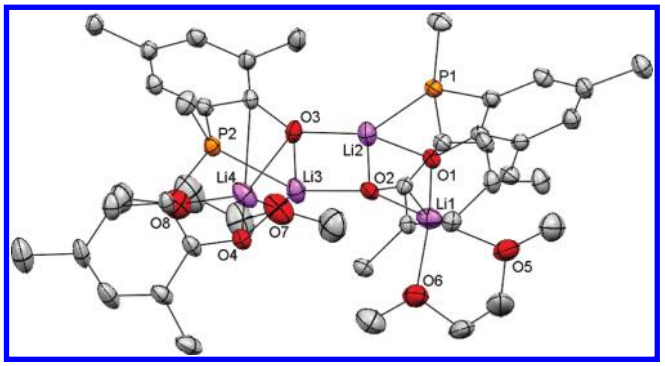

Figure 2. Molecular structure of $\{[^{t}Bu\text{-}OPO]Li_2(DME)\}_2$ with thermal ellipsoids drawn at the 35% probability level. All methyls of the *tert*-butyl groups are omitted for clarity.

reported by Fryzuk et al.; when THF is used in the place of DME for the preparation of [Ph-OPO]Li_2 adducts, coordination of the dative phenolate oxygen to lithium becomes comparable, and thus a dimeric $\{[Ph\text{-}OPO]Li_2(THF)_2\}_2$ is isolable (Figure 3).[31] The distinct conformations of [Ph-OPO]$Li_2(DME)_2$ and $\{[Ph\text{-}OPO]Li_2(THF)_2\}_2$ also underscore the significance of coordinating solvent effect (DME versus THF). Though $\{[^{t}Bu\text{-}OPO]Li_2(DME)\}_2$ and $\{[Ph\text{-}OPO]Li_2(THF)_2\}_2$[31] are conformationally comparable, the three successive Li_2O_2 tetragons comprise an open cubane structure for the former but a ladder configuration for the latter. A similar ladder configuration is also found for $\{[SPS]Li_2(DME)\}_2$ ($[SPS]^{2-}$ = $[PhP(3\text{-}Me_3SiC_6H_3\text{-}2\text{-}S)_2]^{2-}$).[33]

The bond distances and angles of $\{[^{t}Bu\text{-}OPO]Li_2(DME)\}_2$ are essentially similar to those of [Ph-OPO]$Li_2(DME)_2$[13] and $\{[Ph\text{-}OPO]Li_2(THF)_2\}_2$.[31] The phosphorus donor in the monomeric $[^{t}Bu\text{-}OPO]Li_2(DME)$ unit is found to coordinate to only one of the lithium atoms. The slightly shorter P−Li distances in $\{[^{t}Bu\text{-}OPO]Li_2(DME)\}_2$ (2.420(6) and 2.440(6) Å) than $\{[Ph\text{-}OPO]Li_2(THF)_2\}_2$ (2.499(3) Å)[31] are consistent with the stronger electron-releasing nature for the *tert*-butyl substituents. In comparison, the P−Li distance in [Ph-OPO]$Li_2(DME)_2$ is rather longer (2.573(5) Å).[13] As anticipated in view of the inherent geometry imposed by the phosphorus donor, the $[^{t}Bu\text{-}OPO]^{2-}$ ligand adopts a facial coordination mode with respect to Li(2) and Li(3). The geometry of Li(1) and Li(4) is perhaps best described as a distorted tetrahedron with the dihedral angle of two chelating O−Li−O planes being 72.44° and 65.38°, respectively. An additional close contact is also found for these lithium atoms with one of the O-bound aryl carbons (2.513(7) Å for Li(1) and 2.459(8) Å for Li(4)). These distances are well within the sum of lithium and carbon van der Waals radii of 3.45 Å.[34] Interestingly, the coordination geometry of Li(2) and Li(3) is trigonal monopyramidal, with O(2) and O(3) being the corresponding apical donor.

Solution NMR data of $\{[^{t}Bu\text{-}OPO]Li_2(DME)\}_2$ at room temperature are indicative of C_s symmetry for this molecule, suggesting a fluxional process involving presumably the formation of monomeric $[^{t}Bu\text{-}OPO]Li_2(DME)$ via dative O−Li bond dissociation. This hypothesis is in accord with the structurally characterized, mononuclear [Ph-OPO]$Li_2(DME)_2$.[13] The ^1H NMR spectrum exhibits two doublets for aryl protons and two singlets for aryl *tert*-butyls. The integral of DME signals relative to that of $[^{t}Bu\text{-}OPO]^{2-}$ empirically confirms the presence of $\{[^{t}Bu\text{-}OPO]Li_2(DME)\}_2$. In the presence of an excess amount of DME (e.g., 2 equiv), solutions of $\{[^{t}Bu\text{-}OPO]Li_2(DME)\}_2$ exhibit only one set of resonances for DME protons, a result that is ascribable to facile exchange between coordinated and free DME molecules. The coordinated DME in $\{[^{t}Bu\text{-}OPO]Li_2(DME)\}_2$ is thus labile and tends to dissociate. Indeed, standing a C_6D_6 or toluene-d_8 solution of $\{[^{t}Bu\text{-}OPO]Li_2(DME)\}_2$ at room temperature for several hours led to observation of some precipitates. The ^1H NMR spectra of such solutions are too complicated to be interpretable, but are reflective of the formation of C_1-symmetric molecules. We tentatively ascribe this result to, at least in part, the dissociation of one coordinated DME from $\{[^{t}Bu\text{-}OPO]Li_2(DME)\}_2$. Accordingly, the $^{31}P\{^1H\}$ NMR of these C_6D_6 and toluene-d_8 solutions reveals two broad singlets, which, upon addition of an excess amount of DME, merge to give one singlet at −20.7 ppm as what is observed for a freshly prepared sample. Consistently, prolonged heating of solid $\{[^{t}Bu\text{-}OPO]Li_2(DME)\}_2$ under dynamic vacuum to 60 °C for 3 h led to a decrease in coordinated DME, as indicated by ^1H NMR. A variable-temperature $^{31}P\{^1H\}$ NMR study in toluene-d_8 at −80 °C revealed two distinct 1:1:1:1 quartet resonances at −23.3 and −30.1 ppm with coupling constants of 41 and 60 Hz, respectively, indicating the coordination of the soft phosphorus donors to hard, quadrupolar ^7Li atoms (I = 3/2, natural abundance 92.6%). The magnitude of these coupling constants is similar to those found for other lithium phosphine complexes such as $Li[N(o\text{-}C_6H_4PPh_2)_2]$-$(THF)_2$ (34 Hz),[12,35] $[Li(THF)_2][o\text{-}(2,6\text{-}Me_2C_6H_3N)C_6H_4PPh_2]$

(33) Froelich, N.; Hitchcock, P. B.; Hu, J.; Lappert, M. F.; Dilworth, J. R. *J. Chem. Soc., Dalton Trans.* **1996**, 1941–1946.

(34) Huheey, J. E.; Keiter, E. A.; Keiter, R. L. *Inorganic Chemistry: Principles of Structure and Reactivity*, 4th ed.; Harper Collins: New York, 1993.

(35) Liang, L.-C.; Chien, P.-S.; Lin, J.-M.; Huang, M.-H.; Huang, Y.-L.; Liao, J.-H. *Organometallics* **2006**, *25*, 1399–1411.

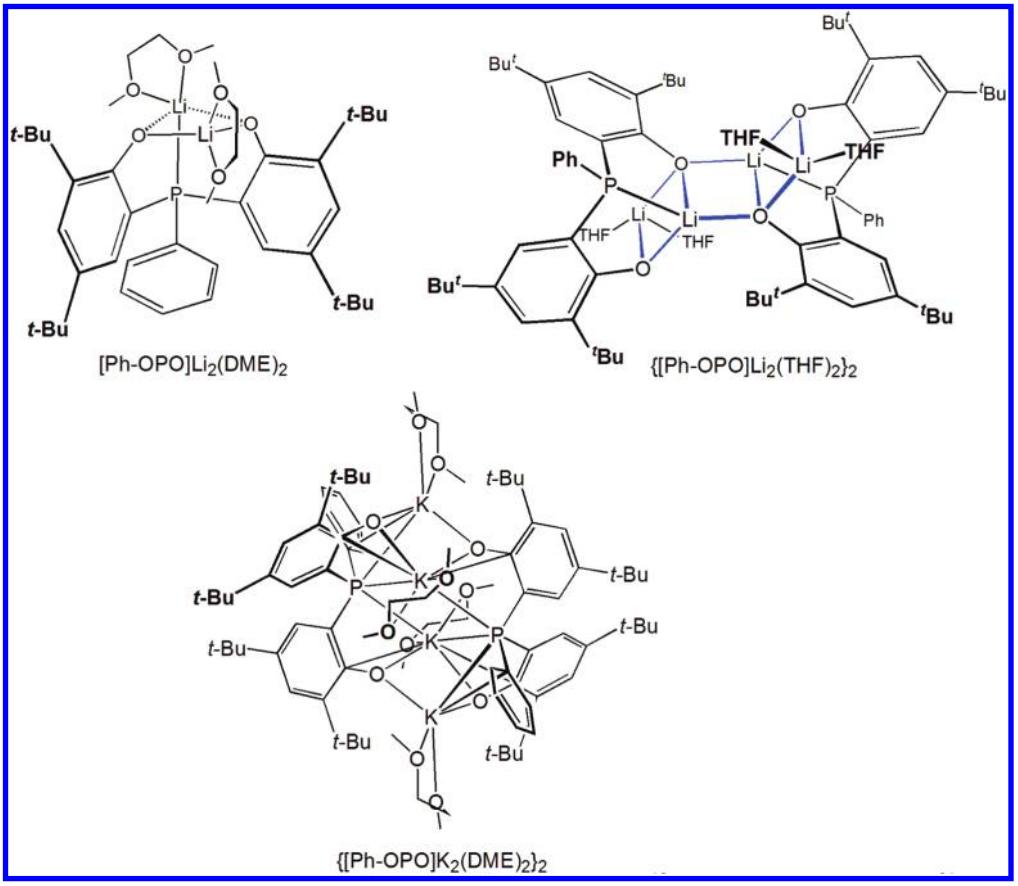

Figure 3. ChemDraw drawings of $[Ph\text{-}OPO]Li_2(DME)_2$,[13] $\{[Ph\text{-}OPO]Li_2(THF)_2\}_2$,[31] and $\{[Ph\text{-}OPO]K_2(DME)_2\}_2$.[13]

Table 2. Selected Bond Distances (Å), Bond Angles (deg), and Torsion Angles (deg) for $\{[^t Bu\text{-}OPO]Li_2(DME)\}_2$

Li(1)−O(1) 1.893(6)	Li(2)−O(2) 2.124(7)	Li(4)−O(4) 1.920(7)
Li(1)−O(6) 2.006(7)	Li(2)−P(1) 2.420(6)	Li(4)−O(7) 2.011(7)
Li(1)−O(2) 2.063(7)	Li(3)−O(2) 1.875(6)	Li(4)−O(8) 2.027(7)
Li(1)−O(5) 2.078(7)	Li(3)−O(4) 1.955(6)	Li(4)−O(3) 2.151(7)
Li(2)−O(3) 1.850(6)	Li(3)−O(3) 2.075(6)	
Li(2)−O(1) 1.909(7)	Li(3)−P(2) 2.440(6)	
O(1)−Li(1)−O(6) 126.9(3)	O(2)−Li(2)−P(1) 82.0(2)	O(7)−Li(4)−O(3) 104.3(3)
O(1)−Li(1)−O(2) 98.7(3)	O(2)−Li(3)−O(4) 139.3(4)	O(8)−Li(4)−O(3) 140.2(4)
O(6)−Li(1)−O(2) 110.0(3)	O(2)−Li(3)−O(3) 101.8(3)	Li(1)−O(1)−Li(2) 86.6(3)
O(1)−Li(1)−O(5) 110.9(3)	O(4)−Li(3)−O(3) 97.8(3)	Li(3)−O(2)−Li(1) 122.8(3)
O(6)−Li(1)−O(5) 79.9(3)	O(2)−Li(3)−P(2) 138.9(3)	Li(3)−O(2)−Li(2) 77.7(2)
O(2)−Li(1)−O(5) 133.8(3)	O(4)−Li(3)−P(2) 78.7(2)	Li(1)−O(2)−Li(2) 77.0(2)
O(3)−Li(2)−O(1) 137.6(4)	O(3)−Li(3)−P(2) 82.2(2)	Li(2)−O(3)−Li(3) 79.5(3)
O(3)−Li(2)−O(2) 100.8(3)	O(4)−Li(4)−O(7) 130.2(4)	Li(2)−O(3)−Li(4) 127.4(3)
O(1)−Li(2)−O(2) 96.1(3)	O(4)−Li(4)−O(8) 110.9(3)	Li(3)−O(3)−Li(4) 77.9(2)
O(3)−Li(2)−P(1) 139.2(3)	O(7)−Li(4)−O(8) 80.2(3)	Li(4)−O(4)−Li(3) 86.6(3)
O(1)−Li(2)−P(1) 81.3(2)	O(4)−Li(4)−O(3) 96.3(3)	
Li(3)−O(3)−Li(2)−O(2) −3.06	Li(3)−O(3)−Li(4)−O(4) 8.63	Li(2)−O(2)−Li(1)−O(1) 9.39

(34 Hz),[36] $[Li(THF)_2][o\text{-}(2,6\text{-}^iPr_2C_6H_3N)C_6H_4PPh_2]$ (38 Hz),[37] $[(2,4,6\text{-}Me_3C_6H_2)NLi\text{-}2\text{-}(4\text{-}MeC_6H_3)]_2PPh(dioxane)$ (40 Hz),[38] $Li[N(o\text{-}C_6H_4P^iPr_2)_2](THF)$ (46 Hz),[35] $Li[N(o\text{-}C_6H_4PCy_2)_2]$-(THF) (48 Hz),[35] $[(Me_2PCH_2)_3CO]Li_3[C(CH_2PMe_2)_3]$ (58 Hz),[39] and the lithium phosphide derivative $[Li(tmeda)]_2[1,2\text{-}C_6H_4(PPh)_2]$ (35 Hz).[40] Consistently, the $^7Li\{^1H\}$ NMR spectrum at −80 °C exhibits two doublet (3.0 ppm, $^1J_{PLi}$ = 60 Hz; 1.6 ppm, $^1J_{PLi}$ = 41 Hz) and two singlet (−0.8 and −0.9 ppm) resonances, confirming the phosphorus donor in each dinuclear unit is bound to one rather than two lithium centers.

The reaction of $H_2[^t Bu\text{-}OPO]$ with an excess amount of NaH in DME at −35 °C afforded quantitatively colorless prisms of $\{[^t Bu\text{-}OPO]Na_2(DME)_2\}_2(\mu\text{-}DME)$ (Scheme 2) suitable for X-ray diffraction analysis. Reminiscent of its lithium analogue, solution NMR data of the sodium complex are consistent with C_s symmetry, with two distinct signals for aryl protons and two for aryl *tert*-butyl groups in the ^1H NMR spectrum. The phosphorus donors resonate at −23.6 ppm.

Figure 4 depicts the molecular structure of $\{[^t Bu\text{-}OPO]Na_2(DME)_2\}_2(\mu\text{-}DME)$. Selected bond distances, bond angles, and

(36) Liang, L.-C.; Lee, W.-Y.; Yin, C.-C. *Organometallics* **2004**, *23*, 3538–3547.
(37) Liang, L.-C.; Lee, W.-Y.; Hung, C.-H. *Inorg. Chem.* **2003**, *42*, 5471–5473.
(38) MacLachlan, E. A.; Fryzuk, M. D. *Organometallics* **2005**, *24*, 1112–1118.
(39) Müller, G.; Feustel, A. *Organometallics* **2003**, *22*, 3049–3058.
(40) Hitchcock, P. B.; Lappert, M. F.; Leung, W.-P.; Yin, P. *J. Chem. Soc., Dalton Trans.* **1995**, 3925–3932.

Scheme 2

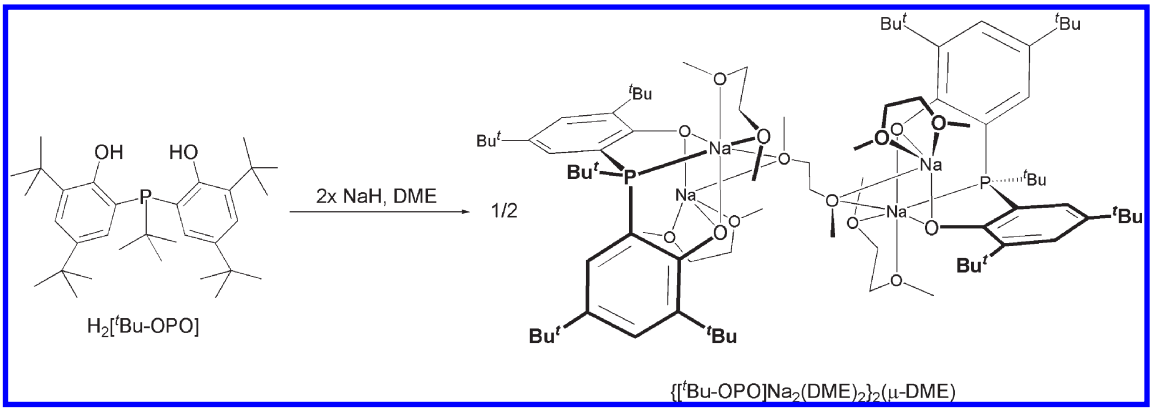

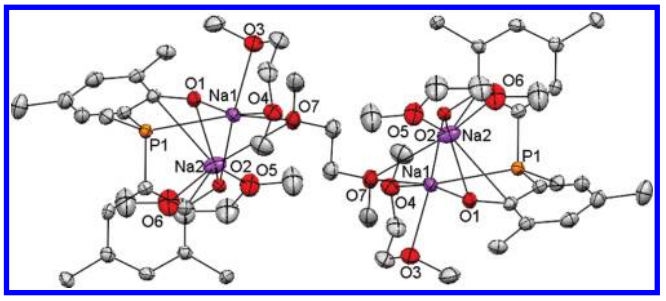

Figure 4. Molecular structure of $\{[^t\text{Bu-OPO}]Na_2(DME)_2\}_2$-($\mu$-DME) with thermal ellipsoids drawn at the 35% probability level. All methyls of the *tert*-butyl groups are omitted for clarity.

torsion angles are summarized in Table 3. As illustrated, this sodium complex contains two $[^t\text{Bu-OPO}]Na_2(DME)_2$ units linked by one bridging DME. The molecule is approximately C_i-symmetric; the inversion center lies at the central point between two methylene carbons in the bridging DME. Each oxygen donor in the bridging DME is bound to both sodium atoms in the $[^t\text{Bu-OPO}]Na_2(DME)_2$ subunit; so are both oxygen donors in $[^t\text{Bu-OPO}]^{2-}$. Interestingly, each $[^t\text{Bu-OPO}]Na_2(DME)_2$ unit is structurally similar to its lithium analogue but adopts one more η^2-DME, consistent with the larger atomic size of the former. In contrast to the nearly planar Li_2O_2 found in monomeric $[^t\text{Bu-OPO}]Li_2(DME)$, the Na_2O_2 moiety in the $[^t\text{Bu-OPO}]Na_2(DME)_2$ subunit adopts a butterfly-like structure. A close contact is also found for Na(2) with both O-bound aryl carbons, where the corresponding distances of 2.975(3) and 2.883(3) Å are well within the sum of sodium and carbon van der Waals radii of 3.95 Å.[34] The coordination number for metallic elements in $\{[^t\text{Bu-OPO}]Na_2(DME)_2\}_2(\mu\text{-DME})$ is thus larger than that for $\{[^t\text{Bu-OPO}]Li_2(DME)\}_2$. The conformation of the $[^t\text{Bu-OPO}]Na_2(DME)_2$ subunit is coincidentally identical to that of the previously established $[\text{Ph-OPO}]Li_2(DME)_2$[13] though the phosphorus substituents incorporated in the biphenolate phosphine ligands are different. The P−Na distance of 2.8757(14) Å is comparable to other phosphine sodium complexes such as $Na_4[^i\text{Pr}_2\text{PCH=C(O)Ph}]_4$ (2.852(2) Å)[41] and $Na_2[(^n\text{Pr}_2\text{P})_2\text{CCH}_2]_2(\text{THF})_6$ (2.9172(16) and 2.9043(16) Å).[42]

Treatment of $H_2[^t\text{Bu-OPO}]$ with an excess amount of KH in DME at −35 °C afforded cleanly the potassium complex, as evidenced by $^{31}P\{^1H\}$ NMR. In contrast to its lighter congeners, attempts to grow X-ray quality crystals of the potassium complex from DME solutions were not successful. Colorless prisms of $\{[^t\text{Bu-OPO}]K_2(THF)_2\}_2$ suitable for X-ray diffraction analysis, however, were isolated in 93% yield after recrystallization from THF solutions (Scheme 3). Surprisingly, DME is not incorporated in this molecule on the basis of X-ray structural investigation, a result that is somewhat consistent with the facile dissociative nature of coordinated DME in $\{[^t\text{Bu-OPO}]Li_2(DME)\}_2$ (vide supra). Instead, the potassium complex contains two coordinated THF molecules per $[^t\text{Bu-OPO}]^{2-}$ ligand, as indicated by ^1H NMR. It is noteworthy that $\{[^t\text{Bu-OPO}]K_2(THF)_2\}_2$ adopts fewer ethereal oxygen donors than the previously established $\{[\text{Ph-OPO}]K_2(DME)_2\}_2$.[13] Reminiscent of lithium and sodium complexes, $\{[^t\text{Bu-OPO}]K_2(THF)_2\}_2$ exhibits solution C_s symmetry on the NMR time scale at room temperature, as evidenced by two distinct signals for aryl protons and two for aryl *tert*-butyl groups in the ^1H NMR spectrum. The phosphorus donors resonate at −17.7 ppm.

The molecular structure of $\{[^t\text{Bu-OPO}]K_2(THF)_2\}_2$ is depicted in Figure 5. Selected bond distances, bond angles, and torsion angles are summarized in Table 4. As illustrated, this molecule contains two $[^t\text{Bu-OPO}]K_2(THF)_2$ units linked with two K−O bridges. The structure is approximately C_i-symmetric, with the inversion center lying at the central point of the bridging K_2O_2 square plane. In comparison, the four potassium atoms in dimeric $\{[\text{Ph-OPO}]K_2(DME)_2\}_2$ are connected by six heteroatoms in two $[\text{Ph-OPO}]^{2-}$ ligands (Figure 3).[13] In contrast to what is found for $\{[^t\text{Bu-OPO}]Li_2(DME)\}_2$ and $\{[^t\text{Bu-OPO}]Na_2(DME)_2\}_2(\mu\text{-DME})$, the two potassium atoms in the monomeric $[^t\text{Bu-OPO}]K_2(THF)_2$ unit are not bridged by both oxygen donors in $[^t\text{Bu-OPO}]^{2-}$. Instead, they are connected by one THF and one oxygen donor in the biphenolate phosphine ligand. Interestingly, one of the aryl rings in $[^t\text{Bu-OPO}]^{2-}$ is π-bound to K(2). The K−C distances (ranging from 3.007(5) to 3.275(5) Å) are comparable to those of $\{[\text{Ph-OPO}]K_2(DME)_2\}_2$ (ranging from 3.126(3) to 3.210(3) Å),[13] $[K(\eta^5\text{-}C_5H_5)]_x$ (ranging from 2.955(5) to 3.140(6) Å),[43] $K(\eta^5\text{-}C_5H_5)$(18-crown-6) (ranging from 2.969(6) to 3.131(7) Å),[44] $[K_4(p\text{-}tert\text{-butylcalix[4]arene-4H})(THF)_5]_2$ (ranging from 3.005(4) to 3.180(4) Å),[45] and $[(THF)_3K][(\mu\text{-}OC_6H_3Me_2\text{-}2,6)_2Y(OC_6H_3Me_2\text{-}2,6)_2(THF)_2]$

(41) Fryzuk, M. D.; Gao, X. L.; Rettig, S. J. *Can. J. Chem.* **1995**, *73*, 1175–1180.
(42) Izod, K.; McFarlane, W.; Tyson, B. V.; Clegg, W.; Harrington, R. W. *Dalton Trans.* **2004**, 4074–4078.
(43) Dinnebier, R. E.; Behrens, U.; Olbrich, F. *Organometallics* **1997**, *16*, 3855–3858.
(44) Neander, S.; Tio, F. E.; Buschmann, R.; Behrens, U.; Olbrich, F. *J. Organomet. Chem.* **1999**, *582*, 58–65.
(45) Gueneau, E. D.; Fromm, K. M.; Goesmann, H. *Chem.—Eur. J.* **2003**, *9*, 509–514.

Table 3. Selected Bond Distances (Å), Bond Angles (deg), and Torsion Angles (deg) for $\{[^t$Bu-OPO$]Na_2(DME)_2\}_2(\mu$-DME)

O(1)−Na(2) 2.273(3)	O(3)−Na(1) 2.424(3)	O(7)−Na(1) 2.461(2)
O(1)−Na(1) 2.340(2)	O(4)−Na(1) 2.460(3)	P(1)−Na(1) 2.8757(14)
O(2)−Na(1) 2.317(2)	O(5)−Na(2) 2.387(3)	
O(2)−Na(2) 2.318(3)	O(6)−Na(2) 2.377(3)	
Na(2)−O(1)−Na(1) 79.70(8)	O(2)−Na(1)−O(4) 101.52(9)	O(4)−Na(1)−P(1) 112.96(7)
Na(1)−O(2)−Na(2) 79.25(8)	O(1)−Na(1)−O(4) 165.59(10)	O(1)−Na(2)−O(2) 94.09(9)
O(2)−Na(1)−O(1) 92.37(8)	O(3)−Na(1)−O(4) 69.71(9)	O(1)−Na(2)−O(6) 114.99(11)
O(2)−Na(1)−O(3) 171.23(10)	O(7)−Na(1)−O(4) 97.63(9)	O(2)−Na(2)−O(6) 118.28(11)
O(1)−Na(1)−O(3) 96.38(9)	O(2)−Na(1)−P(1) 69.31(6)	O(1)−Na(2)−O(5) 124.74(11)
O(2)−Na(1)−O(7) 91.87(9)	O(1)−Na(1)−P(1) 68.33(6)	O(2)−Na(2)−O(5) 134.47(11)
O(1)−Na(1)−O(7) 85.60(8)	O(3)−Na(1)−P(1) 113.51(8)	O(6)−Na(2)−O(5) 69.38(10)
O(3)−Na(1)−O(7) 89.39(9)	O(7)−Na(1)−P(1) 146.36(8)	
Na(1)−O(1)−Na(2)−O(2) 28.48		

Scheme 3

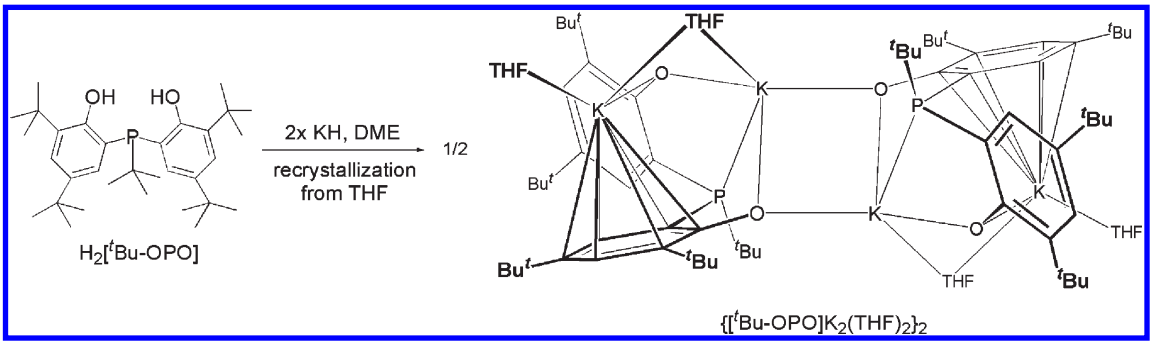

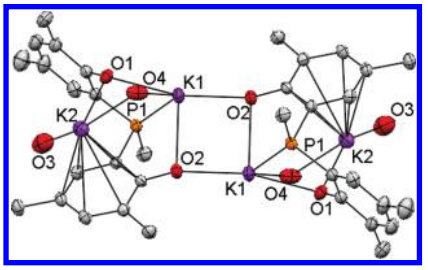

Figure 5. Molecular structure of $\{[^t$Bu-OPO$]K_2(THF)_2\}_2$ with thermal ellipsoids drawn at the 35% probability level. All methyls of the *tert*-butyl groups and methylenes of THF are omitted for clarity.

(ranging from 3.288(9) to 3.400(10) Å).[46] The η^6-coordination for an arene to potassium has also been reported elsewhere.[47−50] The structural discrepancies found for the potassium complex in comparison with its lighter analogues likely reflect the larger atomic size and the preferred π-coordination mode for the former. It is interesting to note that crystallographically characterized potassium complexes of tri(hydrocarbyl)phosphine are extremely rare.[13,51−53] The $[^t$Bu-OPO$]^{2-}$ ligand adopts a facial coordination mode with respect to K(1). The P−K distance of 3.1734(17) Å is notably shorter than those found in $\{[$Ph-OPO$]K_2(DME)_2\}_2$ (3.3853(9), 3.5868(9), and 3.3317(9) Å).[13]

Several phenolate complexes are known to initiate catalytic ROP of heterocyclic molecules.[13,29,54] The catalytic activities of $\{[^t$Bu-OPO$]M_2(solv)_x\}_2$ with respect to ROP of ε-caprolactone (ε-CL) were examined. Preliminary results are summarized in Table 5. Gel permeation chromatography (GPC) analyses of the resulting products reveal a monomodal trace with a reasonably narrow molecular weight distribution ($M_w/M_n < 1.5$) though the measured molecular weights are rather low, particularly that derived from $\{[^t$Bu-OPO$]Na_2(DME)_2\}_2(\mu$-DME). These products are thus best described as oligomers. In contrast, high molecular weight polymers were obtained with catalytic analogues derived from the $[$Ph-OPO$]^{2-}$ ligand.[13] Data listed in entries 1 and 4 highlight the discrepancy between $\{[^t$Bu-OPO$]Li_2(DME)\}_2$ and $[$Ph-OPO$]Li_2(DME)_2$. Nevertheless, the monomer conversions for reactions catalyzed by $\{[^t$Bu-OPO$]M_2(solv)_x\}_2$ are typically high. These results imply that chain transfer reactions frequently occur and concomitantly generate an active, presumably new, species to reinitiate a new propagating chain. It is likely that the identity of the catalytically active species is nearly uniform, though not single-site, as suggested by the measured M_w/M_n values.

Conclusions

We have prepared a series of group 1 metal complexes of $[^t$Bu-OPO$]^{2-}$ and established the solution and solid-state structures of these molecules by multinuclear NMR spectroscopy and X-ray crystallography. These complexes, as elucidated by X-ray diffraction studies, generally constitute two subunits of the type $[^t$Bu-OPO$]M_2(solv)_x$; they are either

(46) Evans, W. J.; Ansari, M. A.; Ziller, J. W.; Khan, S. I. *J. Organomet. Chem.* **1998**, *553*, 141–148.
(47) Chadwick, S.; Englich, U.; Ruhlandt-Senge, K. *Organometallics* **1997**, *16*, 5792–5803.
(48) Hull, K. L.; Carmichael, I.; Noll, B. C.; Henderson, K. W. *Chem.—Eur. J.* **2008**, *14*, 3939–3953.
(49) Gueneau, E. D.; Fromm, K. M.; Goesmann, H. *Chem.—Eur. J.* **2003**, *9*, 509–514.
(50) Frenzel, C.; Jorchel, P.; Hey-Hawkins, E. *Chem. Commun.* **1998**, 1363–1364.
(51) Karsch, H. H.; Graf, V. W.; Reisky, M. *Chem. Commun.* **1999**, 1695–1696.
(52) Gamer, M. T.; Roesky, P. W. *Organometallics* **2004**, *23*, 5540–5544.
(53) Izod, K.; Young, J.; Clegg, W.; Harrington, R. W. *Dalton Trans.* **2005**, 1658–1663.
(54) Chisholm, M. H.; Lin, C.-C.; Gallucci, J. C.; Ko, B.-T. *Dalton Trans.* **2003**, 406–412.

Table 4. Selected Bond Distances (Å), Bond Angles (deg), and Torsion Angles (deg) for $\{[^t\text{Bu-OPO}]K_2(THF)_2\}_2$

O(1)−K(2) 2.596(4)	O(3)−K(2) 2.664(4)	K(1)−O(2)′ 2.545(4)
O(1)−K(1) 2.673(3)	O(4)−K(2) 2.746(4)	K(1)−K(1)′ 3.682(2)
O(2)−K(1)′ 2.545(4)	O(4)−K(1) 2.863(4)	K(1)−K(2) 3.7580(17)
O(2)−K(1) 2.683(4)	P(1)−K(1) 3.1734(17)	
K(2)−O(1)−K(1) 90.99(11)	O(2)′-K(1)−O(4) 116.23(12)	O(4)−K(1)−P(1) 118.58(9)
K(1)′-O(2)−K(1) 89.51(11)	O(1)−K(1)−O(4) 72.68(11)	O(1)−K(2)−O(3) 146.22(14)
K(2)−O(4)−K(1) 84.12(10)	O(2)−K(1)−O(4) 99.60(11)	O(1)−K(2)−O(4) 75.82(11)
O(2)′-K(1)−O(1) 164.82(12)	O(2)′-K(1)−P(1) 121.20(9)	O(3)−K(2)−O(4) 90.15(15)
O(2)′-K(1)−O(2) 90.49(11)	O(1)−K(1)−P(1) 57.27(8)	
O(1)−K(1)−O(2) 100.33(11)	O(2)−K(1)−P(1) 61.33(8)	
K(1)−O(2)−K(1)−O(2) 0.00	O(4)−K(1)−O(1)−K(2) −44.34	

Table 5. Catalytic ROP of ε-CL[a]

entry	initiator	conv (%)[b]	M_n(calc)[c]	M_n(GPC)[d]	M_w/M_n[d]
1	$\{[^t\text{Bu-OPO}]Li_2(DME)\}_2$	100	22.8	2.9	1.44
2	$\{[^t\text{Bu-OPO}]Na_2(DME)_2\}_2$-($\mu$-DME)	94	21.5	0.5	1.48
3	$\{[^t\text{Bu-OPO}]K_2(THF)_2\}_2$	96	21.9	2.5	1.43
4[13]	$[\text{Ph-OPO}]Li_2(DME)_2$[e]	100	22.8	28.5	1.53

[a] Conditions: [initiator] = 1.2 mM, 200 equiv of ε-CL, toluene, 80 °C, 3 h; reaction parameters were not optimized; M_n values are reported in kg mol^{-1} unit. [b] Determined by ^{1}H NMR analysis. [c] Calculated from fw of ε-CL × 200 × conversion, assuming one propagation chain per initiator. [d] Measured by GPC in THF, calibrated with polystyrene standards. [e] [initiator] = 1.4 mM, 12 h.

connected by M−O bridges (M = Li, K) or linked with a μ_2-DME molecule (M = Na). Interestingly, the alkali metal centers within the $[^t\text{Bu-OPO}]Li_2(DME)$ and $[^t\text{Bu-OPO}]Na_2(DME)_2$ subunits are connected by both phenolate oxygen donors in $[^t\text{Bu-OPO}]^{2-}$, whereas those in $[^t\text{Bu-OPO}]K_2(THF)_2$ are linked by one coordinated THF and one phenolate oxygen donor. Of particular note is the construction of an open cubane structure constituted by three fused Li_2O_2 tetragons in $\{[^t\text{Bu-OPO}]Li_2(DME)\}_2$. These structural motifs are notably different from those of analogous compounds derived from a phenylphosphine-bridged biphenolate ligand,[13] a result that is ascribable to the influences induced by distinct phosphorus substituents and coordinating solvents employed. In general, the biphenolate phosphine ligand adopts the anticipated facial coordination mode in all cases. On the basis of the C_s symmetry observed with solution NMR data for all the alkali metal complexes, such a coordination mode appears to be maintained in solution. Variable-temperature $^{31}P\{^1H\}$ and $^7Li\{^1H\}$ NMR studies confirm the coordination of the soft phosphorus donor to the hard lithium center in $\{[^t\text{Bu-OPO}]Li_2(DME)\}_2$. Preliminary catalytic studies reveal that these alkali metal complexes are active initiators for ring-opening oligomerization of ε-CL. Studies involving preparation of transition metal complexes of $[^t\text{Bu-OPO}]^{2-}$ and reaction chemistry derived thereafter will be the subjects of further reports.

Experimental Section

General Procedures. Unless otherwise specified, all experiments were performed under nitrogen using standard Schlenk or glovebox techniques. All solvents were reagent grade or better and purified by standard methods. All other chemicals were obtained from commercial vendors and used as received. The NMR spectra were recorded on Varian Unity or Bruker AV instruments. Chemical shifts (δ) are listed as parts per million downfield from tetramethylsilane and coupling constants (J) and peak widths at half-height ($\Delta\nu_{1/2}$) are in hertz. ^{1}H NMR spectra are referenced using the residual solvent peak at δ 7.16 for C_6D_6. ^{13}C NMR spectra are referenced using the internal solvent peak at δ 128.39 for C_6D_6. The assignment of the carbon atoms is based on the DEPT ^{13}C NMR spectroscopy. ^{31}P and ^{7}Li NMR spectra are referenced externally using 85% H_3PO_4 at δ 0 and LiCl in D_2O at δ 0, respectively. Routine coupling constants are not listed. All NMR spectra were recorded at room temperature in specified solvents unless otherwise noted. Elemental analysis was performed on a Heraeus CHN-O Rapid analyzer.

GPC analyses were carried out at 45 °C on a JASCO instrument equipped with two Waters Styragel HR columns in series and a JASCO RI-2031 refractive index detector. HPLC grade THF was supplied at a constant flow rate of 1.0 mL/min with a JASCO PU-2080 isocratic HPLC pump. Molecular weights (M_n and M_w) were determined by interpolation from calibration plots established with polystyrene standards.

X-ray Crystallography. Data were collected on a Bruker-Nonius Kappa CCD diffractometer with graphite-monochromated Mo Kα radiation (λ = 0.7107 Å). Structures were solved by direct methods and refined by full matrix least-squares procedures against F^2 using WinGX crystallographic software package. All full-weight non-hydrogen atoms were refined anisotropically. Hydrogen atoms were placed in calculated positions. In H_2[Ph-OPO], one *tert*-butyl group is disordered with the methyl substituents being in the ratio of 59:41 over two conformations. The structure of $\{[^t\text{Bu-OPO}]Li_2(DME)\}_2$ contains disordered pentane molecules. Attempts to obtain a suitable disorder model failed. The SQUEEZE procedure of the Platon program[55] was used to obtain a new set of F^2 (*hkl*) values without the contribution of solvent molecules, leading to the presence of significant voids in the structure. The refinement reduced the R1 value to 0.0761. One *tert*-butyl group in $\{[^t\text{Bu-OPO}]Li_2(DME)\}_2$ is disordered with the methyl substituents being in the ratio of 50:50 over two conformations. In $\{[^t\text{Bu-OPO}]Na_2(DME)_2\}_2(\mu\text{-DME})$, two *tert*-butyl groups are disordered with the methyl substituents being in the ratio of 40:60 over two conformations. In $\{[^t\text{Bu-OPO}]K_2(THF)_2\}_2$, one *tert*-butyl group is disordered with the methyl substituents being in the ratio of 52:48 over two conformations. CCDC reference numbers are 777005−777009.

Synthesis of $H_2[^t\text{Bu-OPO}]$. To a diethyl ether solution (20 mL) of 2-bromo-4,6-di-*tert*-butylphenol (4.278 g, 15.0 mmol) at −35 °C was added ^{n}BuLi (12 mL, 2.5 M in hexane, 30.0 mmol). After being stirred at room temperature for 1 h, the solution was cooled to −35 °C again, and a diethyl ether solution (20 mL) of $^t\text{BuPCl}_2$ (1.2 g, 7.5 mmol) at −35 °C was added. The reaction mixture was stirred at room temperature for 12 h and quenched with degassed deionized water (20 mL). The product was extracted with degassed dichloromethane (10 mL × 2). The dichloromethane solutions were combined, dried over $MgSO_4$, and evaporated to dryness under reduced pressure. The residue was dissolved in diethyl ether (3 mL) and MeCN (15 mL) was added to allow for precipitation of the product as an off-white solid; yield 2.17 g (58%). Pale yellow crystals suitable for X-ray diffraction analysis were grown from a concentrated MeCN solution at −35 °C. ^{1}H NMR (C_6D_6, 500 MHz): δ 7.91 (dd, 2, J_{HP} = 4.0, J_{HH} = 2.0, Ar), 7.61 (d, 2, J_{HP} = 12.0, OH), 7.55 (d, 2, $^4J_{HH}$ = 2.0, Ar), 1.54 (s, 18, CMe_3), 1.33 (s, 18, CMe_3),

(55) Spek, A. L. *PLATON-A Multipurpose Crystallographic Tool*; Utrecht University: The Netherlands, 2003.

1.11 (d, 9, $^3J_{HP}$ = 15.0, PC*Me*$_3$). ^{13}C{^{1}H} NMR (C_6D_6, 125.7 MHz): δ 157.87 (d, J_{CP} = 21.12, *C*), 141.99 (d, J_{CP} = 1.76, *C*), 136.31 (d, J_{CP} = 1.76, *C*), 129.25 (d, J_{CP} = 1.89, *C*H), 127.18 (s, *C*H), 116.87 (d, J_{CP} = 6.91, *C*), 35.87 (d, J_{CP} = 2.26, Ar*C*Me$_3$), 34.93 (s, Ar*C*Me$_3$), 32.18 (s, ArC*Me*$_3$), 32.08 (d, $^1J_{CP}$ = 2.26, P*C*Me$_3$), 30.18 (s, ArC*Me*$_3$), 28.66 (d, $^2J_{CP}$ = 12.95, PC*Me*$_3$). ^{31}P NMR (C_6D_6, 202.3 MHz): δ −59.54. Anal. Calcd for $C_{32}H_{51}O_2P$: C, 77.05; H, 10.31. Found: C, 76.97; H, 10.15.

Synthesis of {[^{t}Bu-OPO]Li$_2$(DME)}$_2$. To a prechilled DME solution (6 mL) of H$_2$[^{t}Bu-OPO] (200 mg, 0.4 mmol) at −35 °C was added dropwise *n*-BuLi (0.5 mL, 1.6 M in hexane, 0.8 mmol). The reaction solution was stirred at room temperature for 1 h and filtered through a pad of Celite. All volatiles were removed in vacuo. Pentane (1 mL) was added. The pentane solution was cooled to −35 °C to give the product as colorless prisms suitable for X-ray diffraction analysis; yield 234 mg (98%). ^{1}H NMR (C_6D_6, 500 MHz): δ 7.73 (d, 4, J = 3.0, Ar*H*), 7.45 (d, 4, J = 2.0, Ar*H*), 2.96 (s, 8, OC*H*$_2$), 2.91 (s, 12, OC*H*$_3$), 1.55 (s, 36, ArC*Me*$_3$), 1.46 (d, 18, $^3J_{HP}$ = 13.5, PC*Me*$_3$), 1.38 (s, 36, ArC*Me*$_3$). ^{13}C{^{1}H} NMR (C_6D_6, 125.7 MHz): δ 167.93 (d, J_{CP} = 12.00, *C*), 137.92 (s, *C*), 135.77 (s, *C*), 128.92 (s, *C*H), 125.17 (s, *C*H), 71.41 (s, O*C*H$_2$), 59.42 (s, O*C*H$_3$), 35.80 (s, Ar*C*Me$_3$), 34.64 (s, Ar*C*Me$_3$), 32.52 (s, ArC*Me*$_3$), 31.63 (s, ArC*Me*$_3$), 30.99 (d, J_{CP} = 4.15, P*C*Me$_3$), 30.41 (d, J_{CP} = 14.71, PC*Me*$_3$). ^{31}P{^{1}H} NMR (C_6D_6, 202.3 MHz): δ −20.73. ^{7}Li{^{1}H} NMR (C_6D_6, 194 MHz): δ 0.87. Anal. Calcd for ($C_{72}H_{118}Li_4O_8P_2$)(DME)$_3$: C, 68.52; H, 10.14. Found: C, 68.81; H, 10.54.

Synthesis of {[^{t}Bu-OPO]Na$_2$(DME)$_2$}$_2$(μ-DME). To a prechilled DME solution (8 mL) of H$_2$[^{t}Bu-OPO] (300 mg, 0.6 mmol) at −35 °C was added a prechilled DME suspension (2 mL) of NaH (42 mg, 1.8 mmol). The reaction solution was stirred at room temperature for 1 h and filtered through a pad of Celite. The filtrate was concentrated under reduced pressure until the volume became ca. 1 mL and cooled to −35 °C to give the product as colorless prisms suitable for X-ray diffraction analysis; yield 438 mg (95%). ^{1}H NMR (C_6D_6, 500 MHz): δ 7.62 (s, 4, Ar*H*), 7.45 (s, 4, Ar*H*), 2.95 (s, 20, OC*H*$_2$), 2.85 (s, 30, OC*H*$_3$), 1.60 (s, 36, ArC*Me*$_3$), 1.46 (d, 18, $^3J_{HP}$ = 12.5, PC*Me*$_3$), 1.42 (s, 36, ArC*Me*$_3$). ^{13}C{^{1}H} NMR (C_6D_6, 125.7 MHz): δ 169.91 (d, J_{CP} = 12.82, *C*), 136.92 (s, *C*), 132.95 (s, *C*), 129.78 (s, *C*H), 124.40 (s, *C*H), 71.40 (s, O*C*H$_2$), 59.11 (s, O*C*H$_3$), 35.81 (s, Ar*C*Me$_3$), 34.64 (s, Ar*C*Me$_3$), 32.69 (s, ArC*Me*$_3$), 31.59 (d, J_{CP} = 5.91, P*C*Me$_3$), 30.90 (s, ArC*Me*$_3$), 30.06 (d, J_{CP} = 13.83, PC*Me*$_3$). ^{31}P{^{1}H} NMR (C_6D_6, 202.3 MHz): δ −23.62 ($\Delta\nu_{1/2}$ = 140). With multiple attempts, we were unable to obtain satisfactory data analysis for this compound due likely to the lability of coordinated DME. The NMR spectra are provided in the Supporting Information (Figures S1−S3).

Synthesis of {[^{t}Bu-OPO]K$_2$(THF)$_2$}$_2$. To a prechilled DME solution (4 mL) of H$_2$[^{t}Bu-OPO] (150 mg, 0.3 mmol) at −35 °C was added a prechilled DME suspension (1 mL) of KH (36 mg, 0.9 mmol). The reaction solution was stirred at room temperature for 1 h and filtered through a pad of Celite. All volatiles were removed in vacuo to give {[^{t}Bu-OPO]K$_2$(DME)}$_2$ as an off-white solid; yield 196 mg (98%). The off-white solid was dissolved in THF (1 mL). The THF solution was cooled to −35 °C to give the product as colorless prisms suitable for X-ray diffraction analysis; yield 201 mg (93%, corresponding to the protio ligand employed). ^{1}H NMR (C_6D_6, 500 MHz): δ 7.48 (br s, 4, Ar*H*), 7.32 (s, 4, Ar*H*), 3.42 (m, 16, OC*H*$_2$CH$_2$), 1.60 (s, 36, ArC*Me*$_3$), 1.45 (d, 18, $^3J_{HP}$ = 11.5, PC*Me*$_3$), 1.42 (m, 16, OCH$_2$C*H*$_2$), 1.37 (s, 36, ArC*Me*$_3$). ^{13}C{^{1}H} NMR (C_6D_6, 125.7 MHz): δ 171.06 (br m, *C*), 167.59 (s, *C*), 136.57 (s, *C*), 130.11 (s, *C*H), 125.63 (s, *C*), 123.67 (s, *C*H), 68.11 (s, O*C*H$_2$), 35.94 (s, Ar*C*Me$_3$), 34.56 (s, Ar*C*Me$_3$), 32.78 (s, ArC*Me*$_3$), 31.53 (br s, P*C*Me$_3$), 30.68 (s, ArC*Me*$_3$), 30.37 (d, J_{CP} = 14.20, PC*Me*$_3$), 26.08 (s, OCH$_2$*C*H$_2$). ^{31}P{^{1}H} NMR (C_6D_6, 202.3 MHz): δ −17.72. Attempts to obtain satisfactory analysis data of {[^{t}Bu-OPO]K$_2$(THF)$_2$}$_2$ were not successful. Anal. Calcd for ($C_{32}H_{49}K_2O_2P$)$_2$(DME)$_2$: C, 65.00; H, 8.95. Found: C, 64.71; H, 8.71.

General Procedures for ROP of ε-CL Outlined in Table 5. A toluene solution of {[^{t}Bu-OPO]M$_2$(solv)$_x$}$_2$ (1.2 mM) was added to a toluene solution of ε-CL (200 equiv). Toluene was added, if necessary, to make the total volume of the reaction solution 5 mL. The solution was transferred to a Teflon-sealed reaction vessel and heated to 80 °C for 3 h. After being cooled to room temperature, the reaction solution was quenched with a methanol solution of HCl (1 M). The solution was filtered through a pad of Celite, and all volatiles were removed under dynamic vacuum upon heating until the weights of the resulting viscous residues remained constant.

Acknowledgment. We thank the National Science Council of Taiwan for financial support (NSC 96-2628-M-110-007-MY3, 96-2738-M-110-001, and 96-2918-I-110-011), Ms. Ting-Ting Tsai for preparing NMR samples of {[^{t}Bu-OPO]Li$_2$(DME)}$_2$ in C_6D_6, Mr. Ting-Shen Kuo (NTNU) for assistance with X-ray crystallography, Ms. Ching-Wei Lu (NTU), Ms. I-Chuan Chen (NCHU), and Ms. Chia-Chen Tsai (NCKU) for elemental analysis, Ms. Chao-Lien Ho (NSYSU), Ms. Mei-Yueh Chien (NCHU), and Ms. Ru-Rong Wu (NCKU) for assistance with NMR, Prof. Jyh-Tsung Lee for the access to a GPC instrument, and the National Center for High-performance Computing (NCHC) for accesses to chemical databases. We are also grateful to reviewers for insightful comments.

Supporting Information Available: NMR spectra of {[^{t}Bu-OPO]Na$_2$(DME)$_2$}$_2$(μ-DME) and X-ray crystallographic data in CIF format for H$_2$[^{t}Bu-OPO], H$_2$[Ph-OPO], {[^{t}Bu-OPO]Li$_2$-(DME)}$_2$, {[^{t}Bu-OPO]Na$_2$(DME)$_2$}$_2$(μ-DME), and {[^{t}Bu-OPO]-K$_2$(THF)$_2$}$_2$. This material is available free of charge via the Internet at http://pubs.acs.org.